Synthesis, characterization, biological screenings and interaction with calf thymus DNA as well as electrochemical studies of adducts formed by azomethine [2-((3,5-dimethylphenylimino)methyl)phenol] and organotin(IV) chlorides

Muhammad Sirajuddin [a], Saqib Ali [a,*], Ali Haider [a], Naseer Ali Shah [b], Afzal Shah [a], Muhammad Rashid Khan [b]

[a] Department of Chemistry, Quaid-i-Azam University, Islamabad 45320, Pakistan
[b] Department of Biochemistry, Quaid-i-Azam University, Islamabad 45320, Pakistan

ARTICLE INFO

ABSTRACT

Novel azomethine adducts of Sn(IV) have been synthesized by the reaction of R_nSnCl_{4-n} ($n = 1–3$, R = CH_3, n-C_4H_9, C_6H_5, C_6H_{11}) with 2-((3,5-dimethylphenylimino)methyl)phenol (HL). The products were characterized by elemental analysis, FT-IR, $_1$H, $_{13}$C and $_{119}$Sn NMR spectroscopy. Triphenyltin(IV) chloride [2-((3,5-dimethylphenylimino)methyl)phenol] (**3**) was also characterized by single crystal analysis. Spectroscopic and crystal data suggest that in all the complexes the ligand acts as a monodentate neutral molecule and is coordinated through oxygen to the tin atom forming pentacoordinated tin species. The phenolic hydrogen within the ligand is transferred to the imine nitrogen atom due to the coordination of oxygen with tin after complex formation. The ligand and its complexes have been screened for their biological activities, including DNA interaction, enzymatic, antibacterial, antifungal and cytotoxicity studies. Moreover, the electrochemical behavior of the synthesized compounds was also studied and the results obtained evidenced their irreversible oxidation.

© 2012 Elsevier Ltd. All rights reserved.

1. Introduction

Metal complexes have a massive impact on medicine. They are attractive candidates for the design of new anticancer agents. Cisplatin, carboplatin and oxaloplatin were the first clinically used antitumor drugs. Although platinum based treatment is efficient for several types of solid tumors, their effectiveness is limited by serious nephrotoxicity, myelotoxicity, peripheral neuropathy and tumor resistance. To overcome their clinical problems, a large number of new non-platinum-based anticancer complexes have been screened. Some complexes containing Ti, V, Mo and Ru took the lead in connection with good antitumor activity and remarkably low toxicity. Some diorganotin(IV) complexes were found to have even better activity than cisplatin, which made them suitable candidates for possible clinical use [1].

The chemistry of organotin compounds is gaining paramount attention on account of their interesting structural features [2–4], schizonticidal, antimalarial and fungicidal activities and their potential as agricultural biocides. Organotin compounds have a range of applications, including their use as boat paint additives, to prevent attack by microorganisms, and as insecticides and fungicides; $[(C_4H_9)_3Sn]_2O$ and the water-soluble tributyl mesylimide are widely used as wood preservatives. Several organotin compounds are used commercially as hydrochloric acid scavengers in polyvinyl chloride preparation, and dibutyltin laurate is now a well-established highly effective and universal stabilizer for rigid and flexible PVCs. Organotin species provide excellent protection to the PVC under high thermal stress and confer crystal clarity to the finished article. In relatively recent years, it has been reported that $RSn(SCH_2-COOC_8H_{17})_3$ compounds inhibit dehydrochlorination reactions by exchanging their anionic SR-moiety with the Cl atoms in the polymer [5].

Caution: Nowadays some of these compounds are being banned because of their environmental concerns.

Azomethine ligands are considered as "privileged ligands" due to their ease of preparation and use as fluorogenic agents, pesticides, herbicidal and blocking agents [6]. Coordination of azomethines to organotin(IV) compounds has received considerable attention with respect to their structural variation and potential applications in medicinal chemistry and biotechnology [7–9]. Azomethines in the neutral and deprotonated forms react with organotin(IV) halides, and the complexes formed have been reported to exhibit different modes of coordination [10–17], which may be the cause of their wide applications.

The interaction of organometallic compounds with DNA is of interest for therapeutic treatment as these molecules recognize specific DNA sequences, alter the local DNA structure, inhibit access to the activator or repressor protein and ultimately affect the gene-expression process [18,19]. Most of the chemotherapeutic drugs are DNA-targeted. The binding ability of organotin compounds with DNA depends on the coordination number and nature of the groups bonded to the central tin atom. Small molecules bind to DNA through covalent or non-covalent interactions. Such binding can take place either with the nitrogenous bases or negatively charged oxygen of the phosphate backbone of DNA [20].

In the current article we report the synthesis of an azomethine ligand, [2-((3,5-dimethylphenylimino)methyl)phenol], and its complexes with organotin(IV) compounds. The synthesized ligand and complexes were characterized by various techniques, including FT-IR, NMR, elemental analysis and single crystal analysis. Biological activities including the interaction with DNA, an enzymatic study, antibacterial, antifungal and cytotoxicity of the synthesized ligand and its organotin(IV) complexes were studied. The drug-DNA binding parameters of the synthesized compounds were calculated. The electrochemical behavior of the synthesized compounds was also studied.

2. Experimental

2.1. Materials and methods

The reagents $(CH_3)_3SnCl$, $(n\text{-}C_4H_9)_3SnCl$, $(C_6H_5)_3SnCl$, $(C_6H_{11})_3$ $SnCl$, $(C_4H_9)SnCl_3$ and salicylaldehyde, 3,5-dimethylaniline were obtained from Aldrich (USA) and were used without further purification. All the solvents purchased from E. Merck (Germany) were dried before use according to literature procedures [21]. The melting points were determined in a capillary tube using a Gallenkamp (UK) electrothermal melting point apparatus. IR spectra in the range 4000–100 cm^{-1} were obtained on a Thermo Nicolet-6700 FT-IR spectrophotometer. Microanalysis was done using a Leco CHNS 932 apparatus. ^{1}H and ^{13}C NMR were recorded on a Bruker-300 MHz FT-NMR spectrometer, using CDCl$_3$ as an internal reference [$_1$H (CDCl$_3$) = 7.25 and ^{13}C (CDCl$_3$) = 77]. Chemical shifts are given in ppm and coupling constant (J) values are given in Hz. The multiplicities of the signals in the $_1$H NMR spectra are given with the chemical shifts (s = singlet, d = doublet, t = triplet, q = quartet, quint = quintet, m = multiplet). ^{119}Sn NMR spectra were recorded at 298 K on samples redissolved in DMSO-d_6 with a 400 MHz JEOL ECS instrument. The measurements were recorded at a working frequency of 149.4 MHz and the chemical shifts were referenced to Me$_4$Sn as an external standard. The absorption spectra were measured on a Shimadzu 1800 UV–Vis spectrophotometer. Viscosity was measured by an Ubbelohde viscometer at room temperature. The electrical conductance was measured on a WTW Series Inolab Cond 720. The X-ray diffraction data were collected on a Bruker SMART APEX CCD diffractometer, equipped with a 4 K CCD detector set 60.0 mm from the crystal. The crystals were cooled to 100 ± 1 K using a Bruker KRYOFLEX low temperature device and intensity measurements were performed using graphite monochromated Mo Kα radiation from a sealed ceramic diffraction tube (SIEMENS). Generator settings were 50 kV/40 mA. The structure was solved by Patterson methods and an extension of the model was accomplished by direct methods using the program DIRDIF or SIR2004. Final refinement on F^2 was carried out by full-matrix least squares techniques using SHELXL-97, a modified version of the program PLUTO (preparation of illustrations) and the PLATON package. Voltammetric experiments were carried out using a μAutolab running with GPES 4.9 software, Eco-Chemie, Utrecht, the Netherlands. Measurements were carried out using a glassy carbon working electrode (GCE) with

a geometric area of 0.071 cm^2, a Pt wire counter electrode and a saturated calomel reference electrode (SCE), in a one-compartment electrochemical cell. The GCE was cleaned by polishing with 1 μm alumina paste and rinsed with water before each experiment. 1 mM stock solutions of **1**, **2** and **3** were prepared in 80% ethanol. Compound **3** was used as a representative example of the organotin(IV) complexes of HL. All the experiments were carried out at room temperature (25 ± 1 °C).

2.2. Synthesis

2.2.1. Synthesis of the ligand, 2-((3,5-dimethylphenylimino)methyl) phenol (HL)

Stoichiometric amounts of 3,5-dimethylamine and salicylaldehyde (5 mmol of each) were added to freshly dried toluene. The mixture was refluxed for 3–4 h and the water that formed was removed by using a Dean and Stark apparatus. The solvent was removed by using a rotavapor and the product was obtained in the form of an oily yellow viscous liquid. The chemical reaction is shown in Scheme 1.

Yield: 80%; Molecular formula: C$_{15}$H$_{15}$NO; Mol. wt.: 225; Physical state: Liquid; IR (cm^{-1}) ν: 1664 (C=N), 1404 and 1605 (Ar. C=C), 2865–3017 (broad) (OH), 1572 (CO); ^{1}H NMR (CDCl$_3$, ppm): 2.42 (s, 6H, H1, H1′), 6.99 (s, 1H, H3), 6.96 (s, 2H, H4, H4′), 8.37 (s, 1H, H6), 7.40–7.45 (m, 3H, H10, H11, H12), 7.08–7.11 (d, H9, ^3J[^{1}H–^{1}H] = 8.7 Hz), 13.48 (s, 1H, N···H–O); ^{13}C NMR (CDCl$_3$, ppm): 21.4 (2C, C1, C1′), 139.1 (2C, C2, C2′), 128.7 (1C, C3), 119 (2C, C4, C4′), 148.4 (1C, C5), 161.3 (1C, C6), 117.3 (1C, C7), 162.3 (1C, C8), 132.3 (1C, C9), 119.3 (1C, C10), 133 (1C, C11), 113.1 (1C, C12); Molar Conductance (Λm, S cm^2 mol^{-1}): 15 at 25 °C; Solubility: Chloroform, Ethanol, DMSO, Acetone.

2.2.1.1. General procedure for the synthesis of the organotin(IV) complexes of HL.
Complexes **1**–**5** were prepared by dissolving 1.125 g (5 mmol) of HL in 60 mL freshly dried toluene, followed by the addition of 5 mmol R$_3$SnCl (R = CH$_3$ (**1**), n-C$_4$H$_9$ (**2**), C$_6$H$_5$ (**3**), C$_6$H$_{11}$ (**4**) and C$_4$H$_9$SnCl$_3$ (**5**). The reaction mixture was stirred and refluxed for about 6–7 h. The contents of the flask were then cooled and filtered. The filtrate was rotary evaporated to get the desired product, which was recrystallized in the mixed solvent of chloroform and n-hexane (4:1). The general chemical reaction is shown in Scheme 2.

A trial experiment in the presence of triethylamine was also performed for a comparison of the product with the one prepared without triethylamine. The ligand was taken in freshly dried toluene, to which a stoichiometric amount of triethylamine was added, and the mixture was stirred and refluxed for about 30 min. Then a stoichiometric amount of the organotin compound was added and mixture was again stirred and refluxed for 6–7 h. The contents of the flask were allowed to settle overnight and then they were filtered and rotary evaporated to get the desired product. In the NMR spectrum some extra peaks of triethylamine were observed when compared with the product without triethylamine. From this it was concluded that triethylamine has no role in the adduct formation.

2.2.1.2. Trimethyltin(IV)chloride [2-((3,5-dimethylphenylimino)methyl) phenol] (**1**).
Yield: 83%; Molecular formula: C$_{18}$H$_{24}$ ClNOSn; Mol. Wt.: 424.5; *Anal.* Calc. for C$_{18}$H$_{24}$ClNOSn: C, 50.92; H, 5.70; N, 3.30. Found: C, 51.10; H, 5.90; N, 3.60%. IR (cm^{-1}) ν: 1619 (C=N), 1408 and 1605 (Ar. C=C), 1536 (CO), 2865–3020 (broad, hydrogen bonded OH), 546 (Sn–C), 454 (Sn–O), 303 (Sn–Cl); ^{1}H NMR (CDCl$_3$, ppm): 2.42 (s, 6H, H1, H1′), 6.99 (s, 1H, H3), 6.96 (s, 2H, H4, H4′), 8.63 (s, 1H, H6), 7.40–7.45 (m, 3H, H10, H11, H12), 7.08–7.11 (d, 1H, H9, ^3J[^{1}H–^{1}H] = 9 Hz), 13.52 (s, 1H, N–H···O), 0.71 (s, SnMe), ^2J[$^{117/}$ ^{119}Sn–^{1}H, (57, 59 Hz)]; ^{13}C NMR (CDCl$_3$, ppm): 21.4 (2C, C1, C1′),
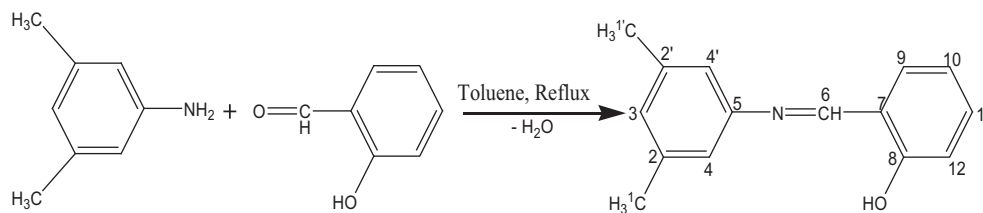
Scheme 1. Structural representation of for the formation of azomethine ligand (HL).

R = Me, n-Bu, Ph, Cy
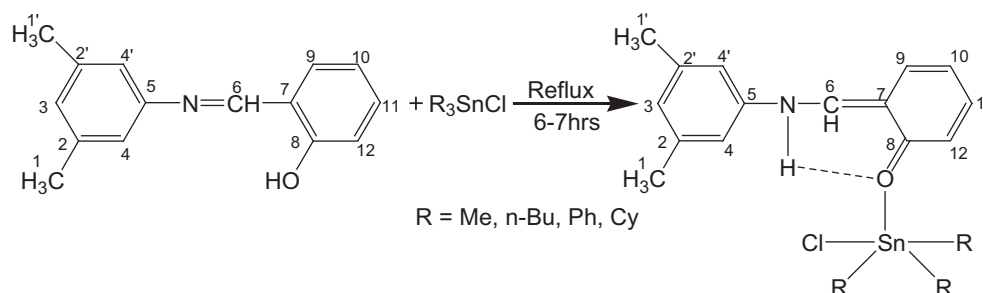
Scheme 2. General structural representation of the organotin(IV) complexes of HL.

139.1 (2C, C2, C2′), 128.7 (1C, C3), 119.1 (2C, C4, C4′), 148.3 (1C, C5), 161.3 (1C, C6), 117.3 (1C, C7), 162.2 (1C, C8), 132.3 (1C, C9), 119.3 (1C, C10), 133 (1C, C11), 113.2 (1C, C12), 21 (s, SnCH$_3$, ^1J[$^{117/119}$Sn–^{13}Cα, (206.3 Hz)]); ^{119}Sn NMR (DMSO, ppm): −222.6; Molar Conductance (Λm, S cm^2 mol^{-1}): 16 at 25 °C; Solubility: chloroform, ethanol, DMSO, acetone.

2.2.1.3. Tri-n-butyltin(IV)chloride [2-((3,5-dimethylphenylimino)methyl) phenol] (**2**). Yield: 80%; Molecular formula: C$_{27}$H$_{42}$ClNOSn; Mol. wt.: 550.79; Physical state: liquid; IR (cm^{-1}) ν: 1621 (C=N), 1413 and 1606 (Ar. C=C), 1540 (CO), 2852–3025 (broad, hydrogen bonded OH), 562 (Sn–C), 455 (Sn–O), 319 (Sn–Cl); ^{1}H NMR (CDCl$_3$, ppm): 2.41 (s, 6H, H1, H1′), 6.97 (s, 1H, H3), 6.95 (s, 2H, H4, H4′), 8.63 (s, 1H, H6), 7.38–7.43 (m, 3H, H10, H11, H12), 7.06–7.09 (d, 1H, H9, ^3J[^{1}H–^{1}H] = 8.4 Hz), 13.46 (s, 1H, N–H···O), {1.81–1.84 (t, Hα), 1.68–1.76 (quint, Hβ), 1.34–1.48 (m, Hγ), 0.98–1.03 (t, Hδ), SnCH$_2$CH$_2$CH$_2$CH$_3$}; ^{13}C NMR (CDCl$_3$, ppm): 21.3 (2C, C1, C1′), 139.1 (2C, C2, C2′), 128.7 (1C, C3), 119.3 (2C, C4, C4′), 148.4 (1C, C5), 161.3 (1C, C6), 119 (1C, C7), 162.2 (1C, C8), 132.3 (1C, C9), 119.3 (1C, C10), 133 (1C, C11), 117.2 (1C, C12), {17.6 (Cα, ^1J[$^{117/119}$Sn–^{13}Cα, (336, 322 Hz)]) 27.9 (Cβ, ^2J[$^{117/119}$Sn–^{13}Cα, (23 Hz)]), 26.9 (Cγ, ^3J[$^{117/119}$Sn–^{13}Cα, (63 Hz)]), 13.7 (Cδ) (SnCH$_2$CH$_2$CH$_2$CH$_3$)}; ^{119}Sn NMR (DMSO, ppm): −220; Molar Conductance (Λm, S cm^2 mol^{-1}): 19 at 25 °C; Solubility: chloroform, ethanol, DMSO, acetone.

2.2.1.4. Triphenyltin(IV)chloride [2-((3,5-dimethylphenylimino)methyl) phenol] (**3**). Yield: 78%; Molecular formula: C$_{33}$H$_{30}$ClNOSn; Mol. wt.: 610.76; m.p: 84–85 °C; *Anal.* Calc. for C$_{33}$H$_{30}$ClNOSn: C, 64.90; H, 4.95; N, 2.29. Found: C, 64.93; H, 4.93; N, 2.30%. IR (cm^{-1}) ν: 1641 (C=N), 1428 and 1607 (Ar. C=C), 1536 (CO), 2853–3064 (broad, hydrogen bonded OH), 565 (Sn–C), 453 (Sn–O), 303 (Sn–Cl); ^{1}H NMR (CDCl$_3$, ppm): 2.4 (s, 6H, H1, H1′), 6.99 (s, 1H, H3), 6.94 (s, 2H, H4, H4′), 8.64 (s, 1H, H6), 7.37–7.43 (m, 3H, H10, H11, H12), 7.07–7.09 (d, 1H, H9, ^3J[^{1}H–^{1}H] = 8.1 Hz), 13.39 (s, 1H, N–H···O), 7.46–7.80 (m, 15H, SnPh); ^{13}C NMR (CDCl$_3$, ppm): 21.3 (2C, C1, C1′), 139.1 (2C, C2, C2′), 128.6 (1C, C3), 119 (2C, C4, C4′), 148.5 (1C, C5), 161.2 (1C, C6), 118.9 (1C, C7), 162.2 (1C, C8), 132.2 (1C, C9), 119.3 (1C, C10), 133 (1C, C11), 117.3 (1C, C12), {139.2 (Cα), 136.2 (Cβ, ^2J[$^{117/119}$Sn–^{13}Cβ, (48.8 Hz)]), 129.2

(Cγ, ^3J[$^{117/119}$Sn–^{13}Cγ, (63 Hz)]), 130.49 (Cδ, ^4J[$^{117/119}$Sn–^{13}Cδ, (12.8 Hz)]) (SnPh)}; ^{119}Sn NMR (DMSO, ppm): −219; Molar Conductance (Λm, S cm^2 mol^{-1}): 18 at 25 °C; Solubility: chloroform, ethanol, DMSO, acetone.

2.2.1.5. Tricyclohexyltin(IV)chloride [2-((3,5-dimethylphenylimino) methyl)phenol] (**4**). Yield: 78%; Molecular formula: C$_{33}$H$_{48}$ClNOSn; Mol. wt.: 628.9; m.p: 108–109 °C; *Anal.* Calc. for C$_{33}$H$_{48}$ClNOSn: C, 63.02; H, 7.69; N, 2.23. Found: C, 63.05; H, 7.66; N, 2.26%; IR (cm^{-1}) ν: 1620 (C=N), 1441 and 1606 (Ar. C=C), 1542 (CO), 2844–2913 (broad, hydrogen bonded OH), 562 (Sn–C), 455 (Sn–O), 319 (Sn–Cl); ^{1}H NMR (CDCl$_3$, ppm): 2.29 (s, 6H, H1, H1′), 6.86 (s, 1H, H3), 6.84 (s, 2H, H4, H4′), 8.64 (s, 1H, H6), 7.41–7.46 (m, 3H, H10, H11, H12), 6.93–6.96 (d, H9, ^3J[^{1}H–^{1}H] = 7.8 Hz), 13.29 (s, 1H, N–H···O), 1.79–1.89 (t, 1H, Hα), 1.53–1.68 (m, 4H, Hβ, Hβ′), 1.53–1.68 (quint, 4H, Hγ, Hγ′), 1.20–1.32 (m, 2H, Hδ); ^{13}C NMR (CDCl$_3$, ppm): 21.3 (2C, C1, C1′), 139.1 (2C, C2, C2′), 128.6 (1C, C3), 119 (2C, C4, C4′), 148.4 (1C, C5), 161.2 (1C, C6), 118.9 (1C, C7), 162.2 (1C, C8), 132.2 (1C, C9), 119.3 (1C, C10), 133 (1C, C11), 117.2 (1C, C12), {33.8 (Cα), ^1J[$^{117/119}$Sn–^{13}Cα, (302, 316 Hz)]; 31.1 (Cβ), ^2J[$^{117/119}$Sn–^{13}Cβ, (65 Hz)]; 28.8 (Cγ), ^3J[$^{117/119}$Sn–^{13}Cγ, (15 Hz)]; 26.8 (Cδ), ^4J[$^{117/119}$Sn–^{13}Cδ, (8 Hz)] (SnCy)}; ^{119}Sn NMR (DMSO, ppm): -223.5; Molar Conductance (Λm, S cm^2 mol^{-1}): 15 at 25 °C; Solubility: chloroform, ethanol, DMSO, acetone.

2.2.1.6. Butyltin(IV)trichloride [2-((3,5-dimethylphenylimino) methyl) phenol] (**5**). Yield: 78%; Molecular formula: C$_{19}$H$_{24}$Cl$_3$NOSn; Mol. wt.: 507.47; m.p.: 102–103 °C; *Anal.* Calc. for C$_{19}$H$_{24}$Cl$_3$NOSn: C, 44.97; H, 4.77; N, 2.76. Found: C, 44.99; H, 4.74; N, 2.69%. IR (cm^{-1}) ν: 1643 (C=N), 1446 and 1589 (Ar C=C), 1551 (CO), 3078–3353 (broad, hydrogen bonded OH), 585 (Sn–C), 454 (Sn–O), 302 (Sn–Cl); ^{1}H NMR (CDCl$_3$, ppm): 2.28 (s, 6H, H1, H1′), 6.97 (s, 1H, H3), 6.81 (s, 2H, H4, H4′), 8.63 (s, 1H, H6), 7.38–7.43 (m, 3H, H10, H11, H12), 7.09–7.12 (d, H9, ^3J[^{1}H–^{1}H] = 8.4 Hz), 13.46 (s, 1H, N–H···O), {1.56–1.60 (t, Hα), 1.76–1.86 (quint, Hβ), 1.33–1.46 (m, Hγ), 0.84–0.88 (t, Hδ), SnCH$_2$CH$_2$CH$_2$CH$_3$}; ^{13}C NMR (CDCl$_3$, ppm): 21.4 (2C, C1, C1′), 139.9 (2C, C2, C2′), 128.6 (1C, C3), 119.2 (2C, C4, C4′), 140.5 (1C, C5), 160.2 (1C, C6), 117.9 (1C, C7), 168.7 (1C, C8), 131.7 (1C, C9), 117.9 (1C, C10), 133 (1C, C11), 115.8 (1C, C12), {25.6 (Cα), 36.2 (Cβ, ^2J[$^{117/119}$Sn–^{13}Cβ, (43 Hz)]),

27.1 (Cγ, ^3J[$^{117/119}$Sn–^{13}Cγ, (90 Hz)]), 13.5 (Cδ) (SnCH$_2$CH$_2$CH$_2$CH$_3$)}; ^{119}Sn NMR (DMSO, ppm): −220.8; Molar Conductance (Λm, Scm^{2}mol^{-1}): 17 at 25 °C; Solubility: chloroform, ethanol, DMSO, acetone.

2.2.2. DNA interaction study by UV–Vis spectroscopy

CT-DNA (20 mg) was dissolved in double deionized water (pH 7.0) and kept at 4 °C for less than 4 days. The nucleotide to protein (N/P) ratio of ~1.9 was obtained from the ratio of absorbance at 260 and 280 nm (A_{260}/A_{280} = 1.9), indicating that the DNA was sufficiently free from protein [22]. The DNA concentration was determined via absorption spectroscopy, using the molar absorption coefficient of 6600 M^{-1}cm^{-1} (260 nm) for CT-DNA [23], and was found to be 2.97×10^{-4}M. Then from this stock solution 10, 15, 20, 25 and 30 μM working solutions were prepared by the dilution method. The compounds were dissolved in 80% ethanol at a concentration of 0.392 mM. The UV absorption titrations were performed by keeping the concentration of the compound fixed while varying the DNA concentration. Equivalent solutions of DNA were added to the complex and reference solutions to eliminate the absorbance of DNA itself. Compound–DNA solutions were allowed to incubate for 30 min at room temperature before the measurements were made. Absorption spectra were recorded using cuvettes of 1 cm path length at room temperature.

2.2.3. Enzymatic activity

2.2.3.1. Assay of alkaline phosphatase inhibition.
The inhibition of alkaline phosphatase was assayed by monitoring the rate of hydrolysis of *p*-nitrophenyl phosphate (*p*NPP) at 25 °C in 0.1 M Na$_2$CO$_3$–NaHCO$_3$ (sodium carbonate–bicarbonate) buffer (pH 10.1) [24,25]. The enzyme catalyzes the hydrolysis of phosphate monoesters, resulting in the formation of inorganic phosphate and an alcohol. The identity of the alcohol varies depending on the specific phosphatase. The assay of alkaline phosphatase activity takes advantage of the fact that the enzyme is non-specific and utilizes the non-biological substrate *p*-nitrophenyl phosphate (colourless) to give the yellow coloured *p*-nitrophenol upon hydrolysis, which helps to monitor the reaction, as shown in Scheme 3 [25].

Stock solutions of 50 μM inhibitors (compounds) in 1 mL DMSO were prepared at room temperature. The buffer and substrate were mixed in 1:4 ratios to make the reagent solution. Then from the reagent solution 2000 μL (2 mL) was taken in the cell, to which 40 μL enzyme and varying concentrations of the inhibitor were added. The activity of the alkaline phosphatase in the presence and absence of inhibitor was measured spectrophotometrically. The release of the yellow coloured *p*-nitrophenol chromophore was monitored at 405 nm wavelength. Enzyme activity has been expressed as the μM of *p*-nitrophenol released per min for 5 min for each concentration of the inhibitor, and then their average value was taken. The inhibition of the enzyme by the inhibitor was calculated by the following formula [26]:

Units/mL enzyme

$$= \frac{\left(\frac{\Delta\ A405\ nm}{min\ Test} - \frac{\Delta\ A405\ nm}{min\ Blank}\right) \text{total VmL(reagent + enzyme + inhibitor)} \times DF}{18.5 \times \text{VmL of enzyme taken}}$$
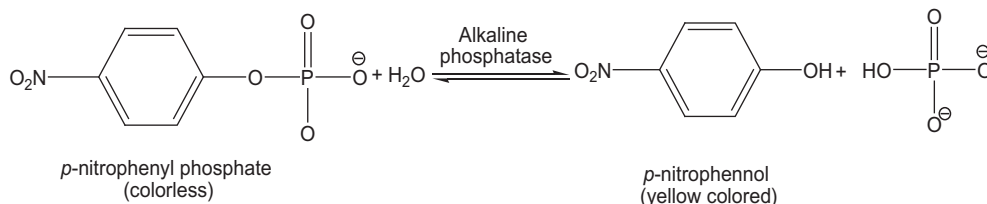
DF = Dilution factor, 18.5 = Millimolar extinction coefficient of *p*-nitrophenol at 405 nm. By the addition of inhibitor the activity of the enzyme decreased, and at higher concentrations it was almost completely inhibited in some cases, as shown in Fig. 8.

2.2.4. Antibacterial assay

The synthesized ligand and its organotin(IV) complexes were tested against six bacterial strains; two Gram-Positive [*Micrococcus luteus* (ATCC10240) and *Staphylococcus aureus* (ATCC6538)] and four Gram-negative [*Escherichia coli* (ATCC15224), *Enterobactor aerogenes* (ATCC13048), *Bordetella bronchiseptica* (ATCC4617) and *Klebsiella pneumoniae* (MTCC618)]. The agar well-diffusion method was used for the determination of antibacterial activity [27]. Broth culture (0.75 mL) containing ca. 10^6 colony forming units (CFU) per mL of the test strain was added to 75 mL of nutrient agar medium at 45 °C, mixed well, and then poured into a 14 cm sterile petri plate. The media was allowed to solidify, and 8 mm wells were dug with a sterile metallic borer. Then a DMSO solution of the test sample (100 μL) at 1 mg/mL was added to the respective wells. DMSO served as a negative control, and the standard antibacterial drugs *Roxyithromycin* (1 mg/mL) and *Cefixime* (1 mg/mL) were used as positive controls. Triplicate plates of each bacterial strain were prepared, which were incubated aerobically at 37 °C for 24 h. The activity was determined by measuring the diameter of the zone showing complete inhibition (mm).

2.2.5. Antifungal assay

Antifungal activity against five fungal strains [*Fusarium moniliformis*, *Aspergillus niger*, *Fusarium solani*, *Mucor species* and *Aspergillus fumigatus*] was determined by using the Agar tube dilution method [27]. Screw caped test tubes containing Sabouraud dextrose agar (SDA) medium (4 mL) were autoclaved at 121 °C for 15 min. The tubes were allowed to cool at 50 °C and non-solidified SDA was loaded with 66.6 μL of compound from the stock solution (12 mg/mL in DMSO) to make a 200 μg/mL final concentration. The tubes were then allowed to solidify in a slanting position at room temperature. Each tube was inoculated with a 4 mm diameter piece of inoculum from seven days old fungal culture. The media supplemented with DMSO and *Turbinafine* (200 μg/mL) were used as a negative and a positive control, respectively. The tubes were incubated at 28 °C for 7 days and growth was determined by measuring the linear growth (mm) and growth inhibition was calculated with reference to growth in the control as shown in the equation below.

$$\% \text{ Growth inhibition} = 100 - \left(\frac{\text{Linear growth in test sample(mm)}}{\text{Linear growth in control(mm)}} \times 100\right)$$

2.2.6. Cytotoxicity

Cytotoxicity was studied by the brine-shrimp lethality assay method [27,28]. Brine-shrimp (*Artemia salina*) eggs were hatched in artificial sea water (3.8 g sea salt/L) at room temperature (22–29 °C). After two days these shrimps were transferred to vials containing 5 mL of artificial sea water (10 shrimps per vial) with 10, 100 and 1000 μg/mL final concentrations of each compound taken from their stock solutions of 12 mg/mL in DMSO. After 24 h,

Scheme 3. The hydrolysis of *p*-nitrophenyl phosphate as catalyzed by alkaline phosphatase.

the number of surviving shrimps was counted. Data was analyzed with a biostat 2009 computer program (Probit analysis) to determine LD_{50} values.

3. Results and discussion

The azomethine, 2-((3,5-dimethylphenylimino)methyl)phenol (HL) was synthesized from the 1:1 condensation of 3,5-dimethylamine and salicylaldehyde. The structural formula with the tautomeric equilibrium is shown in Scheme 4. The new complexes were prepared by the reaction of R_nSnCl_{4-n} ($n = 1–4$, R = CH_3, n-C_4H_9, C_6H_5 and C_6H_{11}) with HL in toluene. The composition of the new compounds was confirmed by their analytical data and the suggested structures were recognized by spectroscopic investigations. The factors behind the selection of azomethines were their ability to exist in keto-enol forms, establish amine-imine equilibria and the presence of a hydrogen bond in the six membered chelate ring. In common solvents, the azomethines exist in appreciable amounts in the ketoenamine (ketamine) form II [29].

3.1. IR spectra

In the infrared spectrum of the free ligand HL, no band was observed in the region (3200–3500 cm^{-1}), attributable to the stretching vibration of free NH or OH groups, indicating intramolecular hydrogen bonding in the ligand. Instead, these bands were shifted to lower frequencies and overlapped with v(C–H) in the range 2865–3017 cm^{-1}. The same behavior was observed in the spectra of the adducts 1–5, which points to the fact that the ring formed by the intramolecular hydrogen bond in the ligand is retained in these adducts. Weak broad bands appearing in the range 2865–3017 cm^{-1} for the free ligand are assigned to v(O–H) and v(N–H), overlapping with v(C–H). These bands were found to shift slightly to higher frequency due to changes in hydrogen bonding and the coordination of the phenolic oxygen atom with tin [30,31]. The shift of a strong band occurring at 1664 cm^{-1}, attributable to v(C=N) in the free ligand, to lower frequency, 1619 (1), 1621 (2), 1641 (3), 1620 (4) and 1643 cm^{-1} (5), indicate adduct formation and proton transfer from the phenolic oxygen atom to the imine nitrogen atom [17]. Further comparison with the spectrum of the free ligand reveals that the band observed at 1572 cm^{-1}, due to CO, shifts to a lower frequency, 1536 (1 and 3), 1540 (2), 1542 (4) and 1551 cm^{-1} (5), providing evidence of the participation of oxygen in bonding with tin and so weakening of the C=O bond [32]. The appearance of new bands observed in the region 546–565 cm^{-1} (v Sn–C) and 453–455 cm^{-1} (v Sn–O), indicate complex formation [33,34]. The bands at 302–319 cm^{-1} were assigned to the Sn–Cl bond [35].

3.2. NMR spectra

The ^{1}H NMR spectrum of the ligand showed the signal of the hydroxyl proton at 13.48 ppm. A pronounced downfield shift is clearly due to strong intramolecular O–H···N hydrogen bonding,

to which the chemical shift of the proton is very sensitive [35]. A notable feature of the ^{1}H NMR spectra of the complexes is the broadening of the phenolic proton peak due to the weakening of the O–H bond and strengthening of the C–N–H hydrogen bond, and so the interaction of the proton signal with the electric quadruple moment of N [36]. No change in the signal attributable to the imine proton (HC=N) in the spectra of both the ligand and complexes indicates that the N atom is not coordinated to tin(IV). No ^nJ(Sn, H) couplings were observed for the n-Bu group and Sn atom due to the complex nature of the protons. The ^{1}H NMR spectrum of 1 showed a singlet at 0.71 ppm (9H) for CH_3–Sn, having a ^2J(^{119}Sn–^{1}H) value (59 Hz) in the range for pentacoordinated trimethyltin(IV) compounds. The ^2J(^{119}Sn–^{1}H) and ^1J(^{119}Sn–^{13}C) heteronuclear coupling values can be used to calculate C–Sn–C angles by using the Lockhart–Manders equations [37,38]. Substitution of the ^2J(^{119}Sn–^{1}H) coupling constant in the equation gives a value of 111.62° for the Me–Sn–Me angle of $Me_3SnClHL$.

The characteristic resonance peaks in the ^{13}C NMR spectra of the complexes were recorded in $CDCl_3$. In the ^{13}C NMR spectrum of the ligand, the peaks at 161.3 and 162.2 ppm belong to the azomethine C-6 and C-8 carbon atoms, respectively. There is no significant change in the chemical shifts of the carbons in the ^{13}C NMR spectra of the complexes compared with the ligand, showing adduct formation. The ^{13}C chemical shift of the *ipso*-carbon of the $SnPh_3$ moiety is around 139.2 ppm in $CDCl_3$ solution, which indicates a five-coordinated triphenyltin centre [39]. Coordination of the tin atom in organotin compounds has been related to the ^1J(^{119}Sn–^{13}C) coupling constants. The ^1J(^{119}Sn–^{13}C) coupling constants for the synthesized compounds are given in Table 1. In the case of the butyl derivatives (compounds 2 and 5), ^2J(^{119}Sn–^{13}C) is smaller than ^3J(^{119}Sn–^{13}C) because ^3J in space can couple more easily to Sn atom than ^2J [40,41].

The ^{119}Sn chemical shift values give information about the environment around the tin atom. All spectra were recorded in DMSO (coordinating solvent). The δ(^{119}Sn) shifts not only depend upon the electron-releasing power of the alkyl and aryl groups, but also on the nature of X in R_nSnX_{4-n}, as the electron-releasing power of the alkyl group increases or the electronegativity of X decreases, the tin atom becomes progressively more shielded and the δ(^{119}Sn) value moves to higher field [40]. A very important property of the ^{119}Sn chemical shift is that an increase in the coordination number of tin from four to five, six or seven usually produces a large upfield shift of δ(^{119}Sn). Holecek et al. and others suggested the δ values from +200 to −60 for four coordinated, −90 to −190 for five-coordinated and −210 to −400 ppm for six coordinated tin atoms relative to tetra-methyltin as a Refs. [42–45].
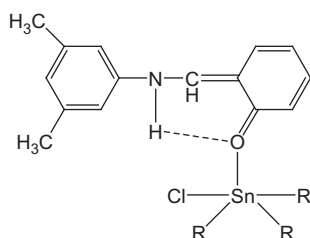
The ^{119}Sn NMR spectra of all the complexes show only a sharp singlet, indicating the formation of a single species. However, these values are strongly dependent on the nature and orientation of the organic groups bonded to tin. The shifts observed in complexes can be explained quantitatively in terms of an increase in electron density on the tin atom as the coordination number increases. The ^{119}Sn chemical shift values measured in coordinating solvent for the synthesized compounds shows penta-coordination around
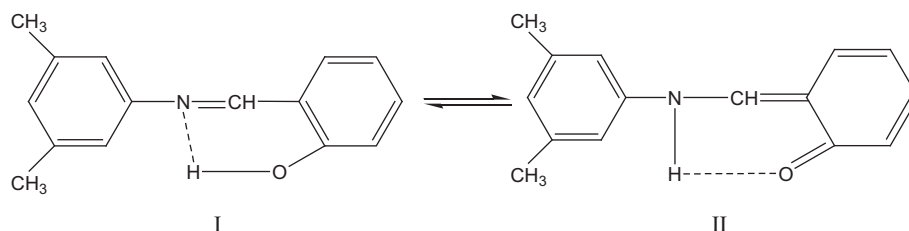
Scheme 4. Possible tautomeric forms for HL.

Table 1
(C–Sn–C) angles (°) based on NMR parameters of selected organotin(IV) derivatives.

Compound	$^1J(^{119}Sn-^{13}C)$ (Hz)	$^2J(^{119}Sn-^{13}C)$ (Hz)	$^2J(^{119}Sn-^{1}H)$ (Hz)	Angle (°)	
				$\theta(1J)$	$\theta(2J)$
1	206.3	–	59.1	95	112
2	336	23	–	111.6	106.2
3	63	–	–	82.3	–
4	315.8	–	–	104.5	–
5	–	40	–	–	106.4

Scheme 5. Structure suggested for the coordination of HL to Sn(IV).

Fig. 1. PLATON diagram of Ph₃SnClHL.

tin, with a trigonal bipyrimidal geometry. It can be inferred from the results that the geometry around tin in the solid and solution state is the same.
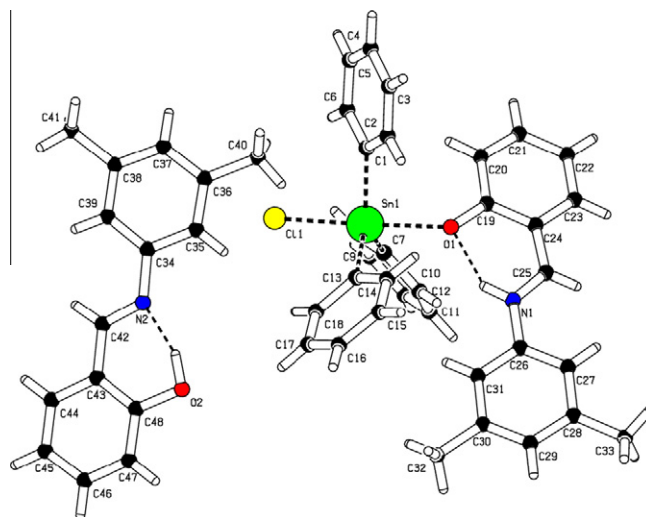
It is concluded that in all the complexes, HL seems to act as a monodentate neutral ligand and coordinates to tin through the oxygen atom, while an intramolecular hydrogen bond still exists between O and N (Scheme 5).

3.3. Crystal structure

The molecular structure of triphenyltin(IV)chloride [2-((3,5-dimethylphenylimino)methyl)phenol] with the crystallographic

Table 2
Crystal data and structure refinement parameters for Ph₃SnClHL (3).

Formula	$C_{33}H_{30}ClN_2O_2Sn$
Formula weight	835.76
Crystal system	monoclinic
Space group	$P21/n$ (no. 14)
a (Å)	17.1699(5)
b (Å)	10.6551(3)
c (Å)	22.5311(7)
α (°)	90
β (°)	91.729(1)
γ (°)	90
V (Å³)	4120.1(2)
Z	4
d (g cm⁻³)	1.348
μ (Mo Kα) (mm⁻¹)	0.725
$F(000)$	1720
Crystal habit/size (mm)	yellow prisms/ 0.36 × 0.25 × 0.23
T (K)	296 (2)
Radiation (Å) (Mo Kα)	0.71073
θ Minimum–maximum (°)	2.44–27.86
Total reflections	9794
Total unique data, R_{int}	36279, 9794, 0.0342
Observed data [$I > 0.0\sigma(I)$]	7413
Nref, Npar	9794, 485
$w = 1/[\sigma^2(Fo)^2+(0.0342P)^2 + 1.1488P]$ where $P = [(Fo)^2 + 2(Fc)^2]/3$	
R, wR_2, S	0.0322, 0.0700, 1.008
Maximum and average shift/error	0.002, 0.00
Minimum and maximum residual Density (e/Å³)	−0.398, 0.317
Goodness-of-fit	1.008

numbering scheme is shown in Fig. 1, while crystal data, selected bond distances and angles are given in Tables 2 and 3, respectively. The complex exists as a monomer. The coordination around the tin centre in the complex is defined by three phenyl groups, one oxygen atom of the phenolic group and one chlorine atom. The geometry around the Sn atom can be determined by the value of $\tau = (\beta - \alpha)/60$, where β is the largest basal angle around Sn and α is the next largest basal angle. The τ value is zero for a perfect square pyramid ($a = \beta = 180°$) and unity for a perfect trigonal pyramidal geometry ($\alpha = 120°$) [46]. The τ value (β = Cl1–Sn1–O1 = 176.49° and α = C–Sn1–C7 = 126.73(8)°) is equal to 0.83, indicating a distorted trigonal bipyramidal geometry around the tin atom. The three phenyl groups are located on the basal plane, occupying the equatorial positions, and the more electronegative O and Cl atoms occupy the axial positions of the trigonal bipyramid [47]. The phenolic oxygen–tin bond distance, 2.3244(14) Å, corresponds to a much weaker interaction, and a similar value of 2.35 Å has been reported for triphenyltin compounds [48]. The hydroxyl H atom is involved in an intramolecular interaction with the imine N atom. Selected bond lengths and bond angles are given in Table 3. Details of the hydrogen bonds are given in Table 4. In the case of the free ligand, the phenolic H atom is attached to the phenolic O atom (enol or imine form) and forms a hydrogen bonding with the imine N atom, while in the case of the complex, the phenolic H atom is transferred to the imine N atom (keto or amine form) and forms a hydrogen bond with the phenolic O atom, as shown in the crystal structure. In the free ligand the N=CH (N2–C42) bond length is 1.274(3) Å, showing double bond character, while in the complex this bond length is increased to 1.300(3) Å (N1–C25), showing single bond character. Also the O2–C48 bond length in the free ligand is 1.369(3) Å, while in the complex this bond length is decreased to 1.312(2) Å (O1–C19), showing double bond character, i.e., the keto form. Thus all this information shows that in the case of the free ligand, the imine form is dominant, while in the case of the adduct, the amine form is dominant. The molecular packing structure is shown in Fig. 2.

3.4. UV–Vis spectroscopy

The interaction of azomethine (HL) and its organotin(IV) complexes with DNA were examined by UV–Vis spectroscopy in order to get some information about their mode of interaction and binding strength. The effect of varying the concentration (10–35 μM) of DNA on the electronic absorption spectra of 0.392 mM of HL and

Table 3
Selected bond lengths (Å) and bond angles (°) for Ph₃SnClHL (**3**).

Bond lengths			
Sn1–O1	2.3244(14)	N1–C26	1.424(3)
Sn1–C1	2.139(2)	N2–C34	1.4200 (16)
Sn1–C7	2.144(2)	C19–C20	1.416(3)
Sn1–C13	2.133(2)	C19–C24	1.416(3)
O1–C19	1.312(2)	C1–C2	1.381(3)
O2–C48	1.369(3)	C24–C25	1.419(3)
N1–C25	1.300(3)	N2–C42	1.274(3)
Bond angle			
O1–Sn1–C1	87.45(6)	Cl1–Sn1–O1	176.49(4)
O1–Sn1–C7	86.32(6)	Cl1–Sn1–C13	96.58(6)
O1–Sn1–C13	86.89(7)	Cl1–Sn1–C7	91.59(6)
C1–Sn1–C7	126.73(8)	Cl1–Sn1–C1	91.56(6)
C1–Sn1–C13	114.97(8)	N1–C25–C24	123.8(2)
C7–Sn1–C13	117.42(8)	N1–C26–C31	117.2(2)
Sn1–O1–C19	127.86(12)	C1–C6–C5	120.8(3)

Table 4
Hydrogen-bond geometries (Å, °) for Ph₃SnClHL (**3**).

D–H···A	D–H	H···A	D···A	D–H···A
N1–H1···O1	0.87(2)	1.86(2)	2.603(2)	142(2)
N2–H2···O2	0.9400	1.7400	2.5989(15)	142(2)

Symmetry codes: (i) $1 - x$, $1 - y$, $-z$; (ii) $-1/2 + x$, $3/2 - y$, $1/2 + z$; (iii) $3/2 - x$, $1/2 + y$, $1/2 - z$.

the organotin(IV) complexes is shown in Figs. 3–6. With an increasing concentration of DNA, the absorption bands of the complexes were affected, resulting in the tendency of hypochromism. The strong absorption of these compounds in the near UV region (319–330 nm) is attributed to the long-living triplet excited state of the aromatic system [49]. The binding of HL, **1**, **2** and **3** to DNA caused hypochromism. A slight bathochromic shift

(~1.2 nm) was observed with increasing concentrations of DNA. These spectral characteristics are indicative of their binding to DNA. Hyperchromic and hypochromic effects are the spectral features of DNA concerning its double-helix structure. These spectral change processes reflect the changes in the conformation and structure of DNA after the complex binds to it [50,51]. Hypochromism results from the contraction of the helix of DNA, as well as from the conformational changes of DNA, while hyperchromism results from damage to the double-helical structure of DNA. In intercalation after binding to DNA, the π^* orbital of the binding ligand could couple with the π orbital of base pairs in the DNA. The coupling π^* orbital is partially filled by electrons, thus decreasing the transition probabilities, and hence resulting in the hypochromicity [52]. These results suggest that HL and its organotin(IV) complexes interact with DNA via the intercalation mode of interaction, since only a hypochromic effect is observed, without any significant changes of shifts in the spectral profiles, which is the indication of a weak interaction with DNA [53]. The stability of the binding properties of the complexes studied towards DNA was examined by taking spectra after 24 and 48 h, and the same results were obtained.

Based upon the variation in absorbance, the association/binding constants of these complexes with DNA were determined according to the Benesi–Hildebrand equation, Eq. (1) [49]:

$$\frac{A_0}{A - A_0} = \frac{\varepsilon_G}{\varepsilon_{H-G} - \varepsilon_G} + \frac{\varepsilon_G}{\varepsilon_{H-G} - \varepsilon_G} \times \frac{1}{K[DNA]} \qquad (1)$$

where K is the association/binding constant, A_0 and A are the absorbances of the drug and its complex with DNA, respectively, and ε_G and ε_{H-G} are the absorption coefficients of the drug and the drug–DNA complex, respectively. The association constants were obtained from the intercept-to-slope ratios of $A_o/(A - A_o)$ versus $1/[DNA]$ plots. The same value of the binding constant was calculated for both the peaks (i.e. 319–324 and 252–253 nm) in all spectra. The
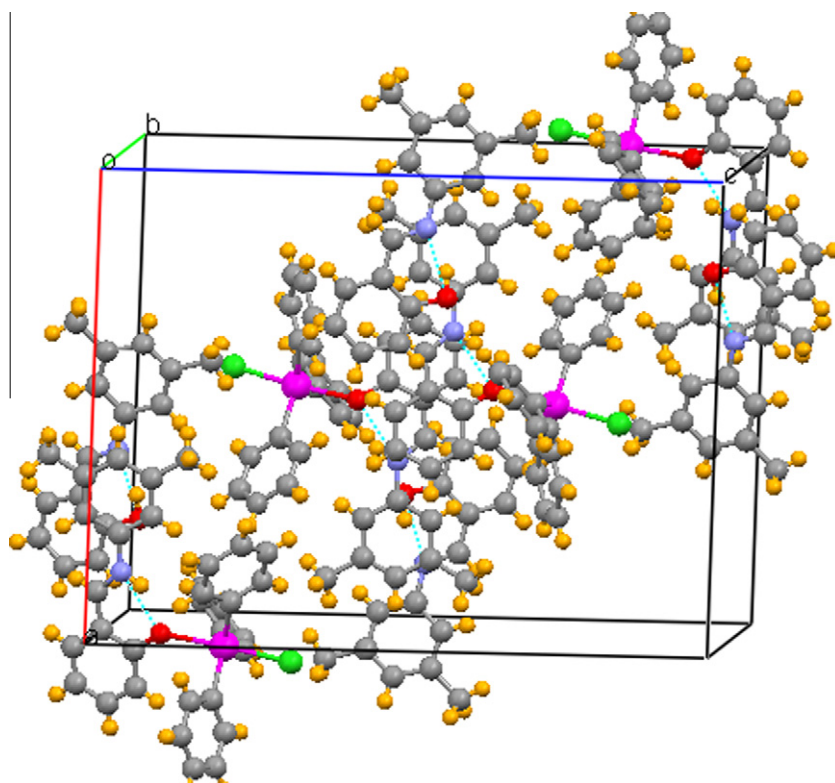

Fig. 2. The molecular packing of Ph₃SnClHL viewed along the *b*-axis. The dotted lines showing the intramolecular H-bonding.
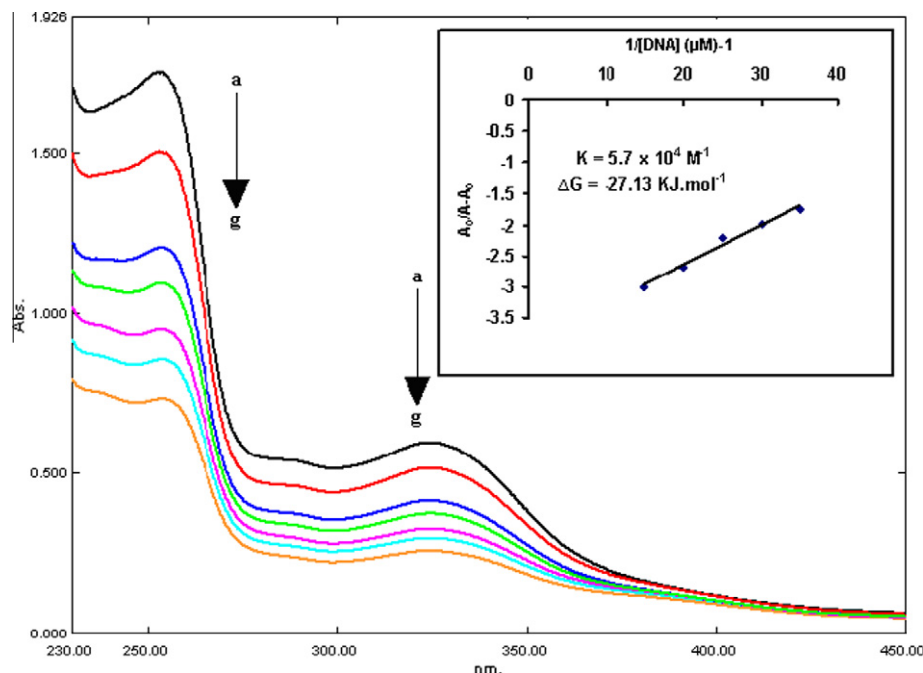
Fig. 3. Absorption spectra of 0.392 mM HL in the absence (a) and presence of 10 μM (b), 15 μM (c), 20 μM (d), 25 μM (e) and 30 μM (f) DNA. The arrow direction indicates increasing concentrations of DNA. The inside graph is the plot of $A_o/(A - A_o)$ vs. 1/[DNA] for the determination of the binding constant and Gibb's free energy of the HL–DNA adduct.
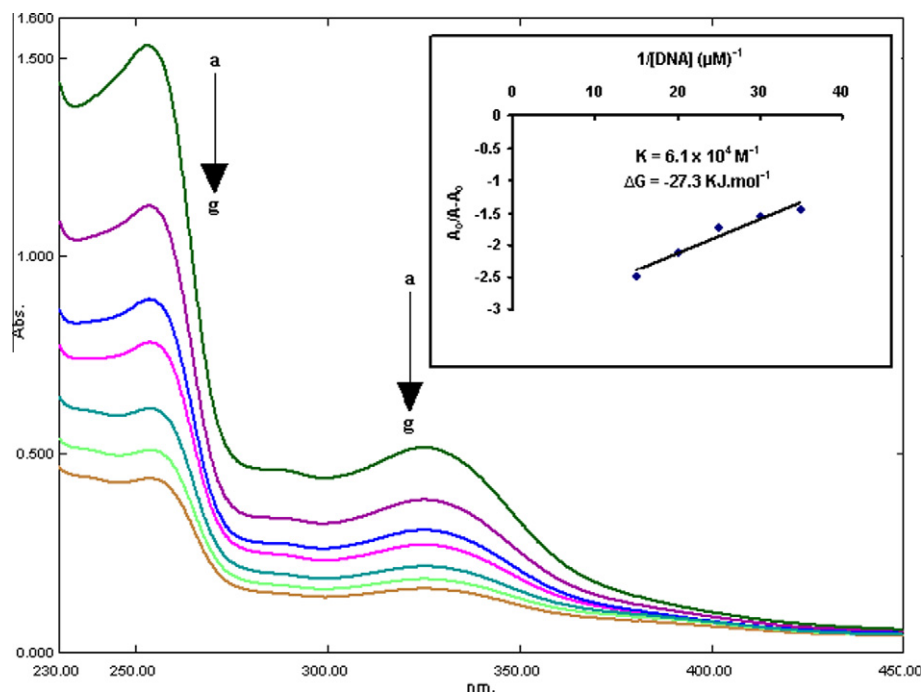

Fig. 4. Absorption spectra of 0.392 mM $(CH_3)_3$SnClHL in the absence (a) and presence of 10 μM (b), 15 μM (c), 20 μM (d), 25 μM (e) and 30 μM (f) DNA. The arrow direction indicates increasing concentrations of DNA. The inside graph is the plot of $A_o/(A - A_o)$ vs. 1/[DNA] for the determination of the binding constant and Gibb's free energy of the $(CH_3)_3$SnClHL–DNA adduct.

binding constant values for HL, **1**, **2** and **3** are 5.7×10^4, 6.1×10^4, 5.6×10^4 and $3.8 \times 10^4 \text{ M}^{-1}$ respectively. The Gibb's free energy (ΔG) was determined from Eq. (2)

$$\Delta G = -RT \ln K \tag{2}$$

where R is general gas constant $(8.314 \text{ JK}^{-1}\text{mol}^{-1})$ and T is the temperature (298 K). The Gibb's free energy (ΔG) values for the HL, **1**, **2** and **3** are -27.13, -27.30, -27.10 and $-26.10 \text{ kJ mol}^{-1}$,

respectively. The negative values of ΔG show that the interaction of these compounds with DNA is a spontaneous process.

3.5. Viscometric studies

The viscometric technique is an effective tool in clarifying the mode of interaction of small molecules with DNA. The viscosity of DNA is sensitive to DNA length change, therefore its measurement
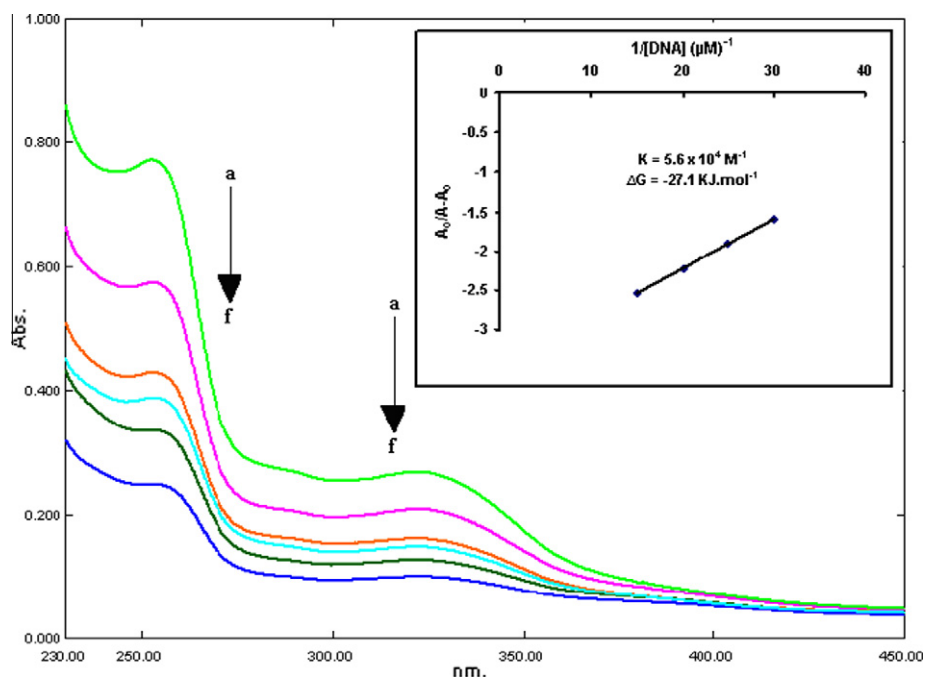
Fig. 5. Absorption spectra of 0.392 mM (C$_4$H$_9$)$_3$SnClHL in the absence (a) and presence of 10 μM (b), 15 μM (c), 20 μM (d), 25 μM (e) and 30 μM (f) DNA. The arrow direction indicates increasing concentrations of DNA. The inside graph is the plot of $A_o/(A - A_o)$ vs. 1/[DNA] for the determination of the binding constant and Gibb's free energy of the (C$_4$H$_9$)$_3$SnClHL–DNA adduct.

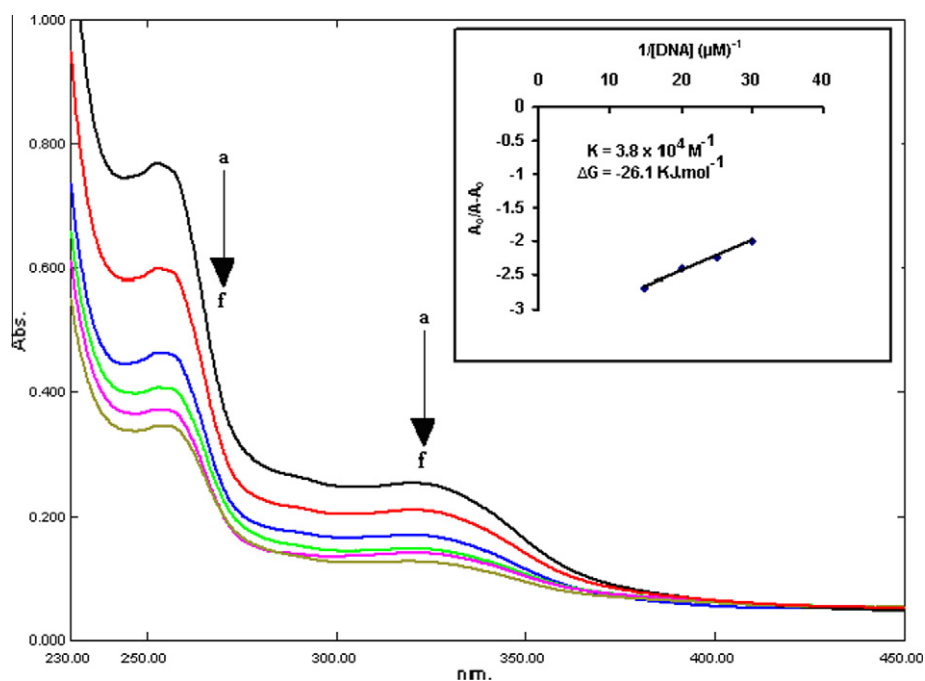**Fig. 6.** Absorption spectra of 0.392 mM (C$_6$H$_5$)$_3$SnClHL in the absence (a) and presence of 10 μM (b), 15 μM (c), 20 μM (d), 25 μM (e) and 30 μM (f) DNA. The arrow direction indicates increasing concentrations of DNA. The inside graph is the plot of $A_o/(A - A_o)$ vs. 1/[DNA] for the determination of the binding constant and Gibb's free energy of the (C$_6$H$_5$)$_3$SnClHL–DNA adduct.

upon addition of a compound is often considered the least ambiguous and most critical method to clarify the interaction mode of a compound with DNA and provides reliable evidence for the intercalative binding mode. Relative viscosity measurements have proved to be a reliable method for the assignment of the mode of binding compounds to DNA. In the case of classic intercalation, DNA base pairs are separated in order to host the bound compound, resulting in the lengthening of the DNA helix and subsequently increased DNA viscosity. On the other hand, the binding of a compound exclusively in DNA grooves by means of partial and/or non-classic intercalation, under same conditions, (e.g., netropsin, distamycin), causes a bend or kink in the DNA helix, reducing its effective length
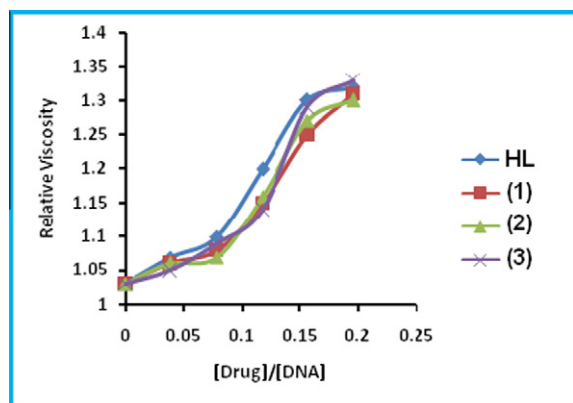
Fig. 7. Effects of the increasing amount of HL, and compounds **2** and **3** on the relative viscosity of CT-DNA at 25 ± 0.1 °C. [DNA] = 2.97 × 10⁻⁴ M.

and, as a result, the DNA solution's viscosity is decreased or remains unchanged, i.e. groove binders and electrostatic interaction do not lengthen the DNA molecules [54–57].

A series of solutions were made with a constant concentration of DNA (2.97×10^{-4} M) and varying the concentration of compounds HL, **1**, **2** and **3**. All of the samples were allowed to equilibrate for 10 min prior to the flow time measurement. The values of the relative viscosity (η/η_o)$^{1/3}$ were calculated from (t/t_o)$^{1/3}$ ratio for all samples, where t, t_o, η and η_o represent the time and viscosity of the DNA solution with and without compound respectively. (η/η_o)$^{1/3}$ was plotted versus the [compound]/[DNA] ratio (Fig. 7), which shows that the viscosity increases upon the addition of increasing amounts of the compounds, therefore the intercalation mode is selected for the interaction of HL, **1**, **2** and **3** with DNA.

3.6. Enzymatic study

The effect of various concentrations of HL and its organotin(IV) complexes on the activity of the enzyme Alkaline Phosphatase EC 3.1.3.1 was studied for the hydrolysis of pNPP. Alkaline Phosphatases catalyze the transfer of phosphate groups to water (hydrolysis) or alcohol (transphosphorylation) using a wide variety of phosphomonoesters and are characterized by a high pH optima and a broad substrate specificity [58]. From the study, we have observed that the presence of HL and its organotin(IV) complexes results in the deactivation of the enzyme. The activity of the enzyme

was markedly decreased by increasing the concentration of HL and its organotin(IV) complexes, and it was almost completely lost at high concentration. The remarkable activity of the ligand may be due to the OH group, which can play an important role in the enzymatic activity [59]. Among the studied azomethine and its organotin(IV) complexes, the highest activity was exhibited by the Ph₃Sn(IV) derivative. The lower activity of the organotin(IV) complexes (except for triphenyltin(IV)) is most probably be due to the formation of a stable bond upon complexation between the tin and oxygen atoms. The different behavior of the triphenyltin(IV) complex can be due to weaker interactions of ligand with tin because of the bulky phenyl groups, thereby regulating the formation of the R₃Sn+(IV) moiety [60] which plays a key role in the inhibition of the alkaline phosphatase enzyme. The inhibition profile is shown in Fig. 8.

3.7. Antimicrobial activity and cytotoxicity

In vitro biological screening tests of the synthesized ligand and its organotin(IV) complexes were carried out for antibacterial activity. The experiment was performed in triplicate using the agar well-diffusion method. *Roxyithromycin* and *Cefixime* were used as positive controls. The criteria for activity is based on the zone of inhibition (mm); an inhibition zone of more than 20 mm shows significant activity, for an 18–20 mm zone the inhibition activity is good, 15–17 mm is low, and below 11–14 mm is non-significant activity. The antibacterial study demonstrates that all compounds, except the ligand and compound **1**, have activity toward the tested bacteria. Complex **3**, showed significant activity against three pathogenic strains, *S. aureus*, *M. luteus* and *B. bronchiseptica*, **5** showed significant activity against four strains, *S. aureus*, *M. luteus*, *E. coli* and *B. bronchiseptica*, where the activity exhibited against *E. coli* is better than *Cefixime*, used as positive control. Complex **2** showed low to good activity against all pathogenic strains. Complex **4** showed non-significant to good activity against all tested strains. The results are shown in Table 5.

The synthesized ligand and its organotin(IV) were also subjected to antifungal activity tests against five fungal strains [*Alternaria species*, *A. niger*, *F. solani*, *Mucor species* and *A. fumigatus*] by using the Agar tube dilution method. The results are shown in Table 5. *Terbinafine* was used as a standard drug in this assay. The criteria for activity is based on percent growth inhibition; more than 70% growth inhibition was considered as significant activity, 60–70% inhibition activity was good, 50–60% inhibition activity was moderate, while below 50% inhibition activity was
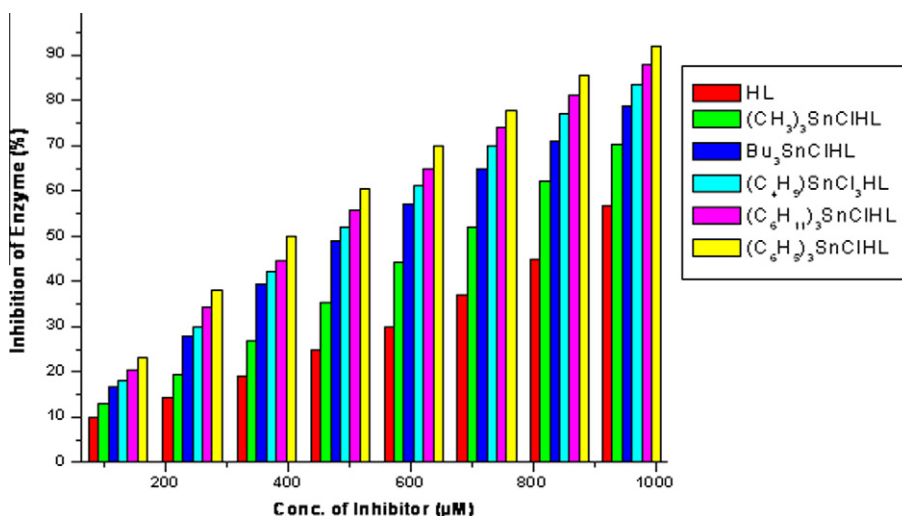

Fig. 8. Bar graphical representation of the inhibition of ALP by HL and its organotin(IV) complexes.

considered as non-significant. The results show that the synthesized organotin(IV) complexes in general have more activity than the ligand, except in few cases. Complex **2** shows 100% growth inhibition against all tested fungal strains, like the reference drug *Terbenafine*. Similarly complexes **3** and **4** showed significant inhibiting activity against all strains, but less than compound **2**. Complexes **1** and **5** showed no to good activity against the tested strains.

The antimicrobial activity of the azomethines expressed a considerable enhancement on coordination with the metal ions. This increase in the activity may be due to the fact that their structures mainly possess an additional C=N bond. It has been reported earlier that azomethines with nitrogen and oxygen donor systems inhibit enzyme activity since the enzymes, which require these groups for their activity, appear to be especially more susceptible to deactivation by metal ions on coordination.

Though the exact biochemical mechanism is not completely understood, the mode of action of antimicrobials may involve various targets in the microorganisms. These targets include the following:

(i) The higher activity of the metal complexes may be due to the different properties of the metal ions upon chelation. The polarity of the metal ions will be reduced due to the overlap of the ligand orbitals and partial sharing of the positive charge of the metal ion with donor groups. Thus, chelation increases the penetration of the complexes into the lipid membranes and the blockage of metal binding sites in the enzymes of the microorganisms [61].

(ii) Tweedy's chelation theory predicts that chelation reduces the polarity of the metal atom, mainly because of partial sharing of its positive charge with donor groups and possible electron delocalization over the entire ring. This consequently increases the lipophilic character of the chelates, favoring their permeation through the lipid layers of the bacterial membrane [62].

(iii) Interference with the synthesis of cellular walls, causing damage that can lead to altered cell permeability characteristics or disorganized lipoprotein arrangements, ultimately resulting in cell death.

(iv) Deactivation of various cellular enzymes that play a vital role in the metabolic pathways of these microorganisms.

(v) Denaturation of one or more cellular proteins, causing the normal cellular processes to be impaired.

(vi) Formation of a hydrogen bond through the azomethine group with the active centers of various cellular constituents, resulting in interference with normal cellular processes [63].

(vii) Inhibition of the replication of DNA by interacting with the enzyme prosthetic group (non-protein group) [64].

The cytotoxicity was studied by the brine-shrimp lethality method and the results are summarized in Table 6. The LD_{50} data show that all the tested compounds, even the ligand, are toxic with LD_{50} values in the range 0.42–44.55 µg/mL in comparison to the reference drug MS-222 (*Tricaine Methanesulfonate*) with an LD_{50} value of 4.3 µg/mL. Complexes **1**, **3** and **5** were the most toxic as compared to the tested compounds and reference drugs.

3.8. Conductometric study

The conductance of the synthesized ligands and complexes in 80% ethanol at 25 °C falls in the range of 15–19 $S\,cm^2\,mol^{-1}$, suggesting their non-electrolytic nature [65]. This shows that they are stabile and hence do not undergo ionization.

3.9. Electrochemical characterization

The redox behaviour of 0.5 mM **1**, **2** and **3** was studied by cyclic voltammetry (CV) at 100 mV s^{-1} scan rate in a N$_2$ saturated solution of 80% ethanol. The CV's were initially started at +0.00 V and recorded between potential limits of +1.50 and −1.00 V (Fig. 9A). On the 1st voltammogram, started in the positive direction, one oxidation peak was observed showing that compound **3** is oxidizable under these conditions. No corresponding peak was observed in the reverse scan, which indicates that the oxidation product of compound **3** is not reducible. The same response was also shown by **1** and **2**. The absence of a peak on the cathodic part of the voltammograms indicates the stability of the Sn(IV) oxidation state in all cases. Therefore, for the oxidation of these complexes, CV's were always recorded in the positive going direction from 0.00 to 1.00 V.

The first scan CV's of 0.5 mM **1**, **2** and **3** (shown in Fig. 9B) registered single irreversible oxidation peaks at 0.73, 0.60 and 0.78 V. The anodic peaks of these complexes are attributed to the oxidation of the –N=CH– group. The attribution is strengthened by the appearance of irreversible anodic peak in the same CV region of guanine due to the oxidation of the –N=CH– group, as reported by earlier electrochemists [65,66]. The higher oxidation potential

Table 5
Antimicrobial Activity of HL and its organotin(IV) compounds.

Compound no.	Antibacterial						Antifungal				
	Average zone of inhibition(mm) inhibition ± SD						Mean value of percent growth inhibition ± SD				
	S. aureus	K. pneumonia	M. luteus	E. aerogenes	E. coli	B. brochiseptica	A. Flavus	F. solani	A. niger	Mucor sp.	A. fumigatus
HL	–[a]	–	–	–	–	–	–	91 ± 0.5	62 ± 0.4	60 ± 0.4	–
1	–	–	–	–	–	–	35 ± 0.24	–	79 ± 0.6	59 ± 0.5	10 ± 0.9
2	19.5 ± 0.2	15 ± 0.23	20 ± 0.21	14.5 ± 0.2	19 ± 0.24	19 ± 0.24	100	100	100	100	100
3	30 ± 0.23	15 ± 0.34	24 ± 0.21	16 ± 0.22	17 ± 0.12	21 ± 0.24	100	99 ± 0.5	98 ± 0.4	98 ± 0.5	100
4	15 ± 0.25	12 ± 0.3	16 ± 0.26	14 ± 0.27	17 ± 0.02	18 ± 0.19	95 ± 0.23	80 ± 0.8	95 ± 0.2	99 ± 0.1	100
5	22 ± 0.22	15 ± 0.75	24 ± 0.26	19 ± 0.25	30 ± 0.21	21 ± 0.27	25 ± 0.69	–	69 ± 0.2	35 ± 0.6	55 ± 0.19
Roxythromycin[b]	36 ± 0.42	26 ± 0.23	35 ± 0.26	20 ± 0.25	26 ± 0.20	35 ± 0.3	*[d]	*	*	*	*
Cefixime[b]	22 ± 0.02	21 ± 0.020	30 ± 0.024	16 ± 0.025	22 ± 0.024	26 ± 0.02	*	*	*	*	*
Terbinafine[c]	*	*	*	*	*	*	100	100	100	100	100

[a] Show no activity.
[b] Reference drug, *Roxythromycin* and *Cefixime* 1 mg/ml for antibacterial activity.
[c] Reference drug, *Terbinafine* for antifungal activity.
[d] No activity. SD = Standard deviation. % inhibition of fungal growth = $100 - g_t/g_c \times 100$ where g_t = linear growth in test (mm) and g_c = linear growth in vehicle control (mm).

Compound	No. of shrimps killed out of 30 per dilution[a]			LD$_{50}$[b,c]
	1000 µg/ml	100 µg/ml	10 µg/ml	
HL	29	24	3	44.55
1	30	27	25	0.42
2	30	30	25	5.05
3	30	27	23	1.46
4	30	30	19	8.24
5	30	24	22	1.89
Vehicle control	0	0	0	

[a] Against brine-shrimps (in vitro).
[b] Data is based on mean value of three replicates each of 10, 100 and 1000 µg/mL.
[c] Compared to standard drug MS-222 (Tricaine methanesulfonate) with LD$_{50}$ value of 4.30 µg/mL.

of **3** indicates that it is difficult to oxidize as compared to **1** and **2**. The abstraction of an electron from the imine group is made difficult by the involvement of the lone pair of electrons of N in hydrogen bonding with the hydrogen of the phenolic group. The result is also supported by crystallography, NMR and IR spectroscopy. The higher peak current of **1** can be linked to its greater mobility as its molecular mass is lower than that of **2** and **3**. On recording successive scans in the same solution, without cleaning the electrode surface, a decrease in the peak currents of all the complexes was observed. The 1st and 2nd scan CV's of 0.5 mM **1** are shown in Fig. 9C. The decrease in peak currents can be explained by the adsorption of **1** oxidation products at the GCE surface, which lowers the available electrode surface area. CVs were also obtained at different scan rates in a N$_2$ saturated solution of 0.5 mM **3**. With the increase in scan rate, a slight shift of the peak potential to more positive values was observed.

The difference between the peak potential E_{pa} and the potential at peak half height $E_{pa/2}$ was $|E_{pa} - Ea_{pa/2}|$ ~95 mV. Since for a diffusion-controlled irreversible system $|E_{pa} - E_{pa/2}| = 47.7/(\alpha_a n)$, where α_a is the anodic charge transfer coefficient and n the number of electrons in the rate-determining step [67], $\alpha_a n = 0.50$ was calculated. The peak current in amperes for an irreversible system is given by $I_{pc}(A) = 2.99 \times 10^5 n (\alpha_a n)^{1/2} A [O]_\infty D_O^{1/2} v^{1/2}$ where n is the number of electrons transferred during the oxidation, v is the number of scans, A is the electrode area in cm^2, D_O is the diffusion coefficient in cm^2 s^{-1}, $[O]_\infty$ is the concentration in mol cm^{-3} and v is in V s^{-1} [68]. By plotting I_{pc} versus $v^{1/2}$, assuming $n = 1$ for **3** the value of D_O was obtained as 3.17×10^{-6} cm^{2}s^{-1}. Similarly the values of the diffusion coefficient for **1** and **2** were calculated as 8.58×10^{-6} and 5.33×10^{-6} cm^2 s^{-1}, respectively. The lower D_O value of **3** corresponds to its slower mobility due to its greater molecular mass.

The cyclic voltammetric behavior of 0.5 mM **3** in the absence and presence of 50 µM DNA at a bare GCE is shown in Fig. 9D. The voltammogram of **3** in the presence of DNA registered a decrease in peak current. The rationale behind the diminution in peak current is the probable decrease in the concentration of free **3** due to the formation of a macromolecular **3**-DNA complex. The interaction of **3** with DNA is expected to cause an alteration in the DNA copying machinery that may stop the proliferation of cancerous cells. Similar behavior was observed for **1** and **2**. The weak current signals and noise could not allow for quantitative measurements.

4. Conclusion

The ligand 2-((3,5-dimethylphenylimino)methyl)phenol and its organotin(IV) complexes were successfully synthesized and characterized. The ligand was treated with different organotin(IV) chlorides to form the corresponding complexes. It may be concluded that the ligand coordinates through oxygen to the Sn atom, leading to the formation of a five coordinated tin species. The synthesized compounds show moderate antimicrobial and cytotoxic activities.
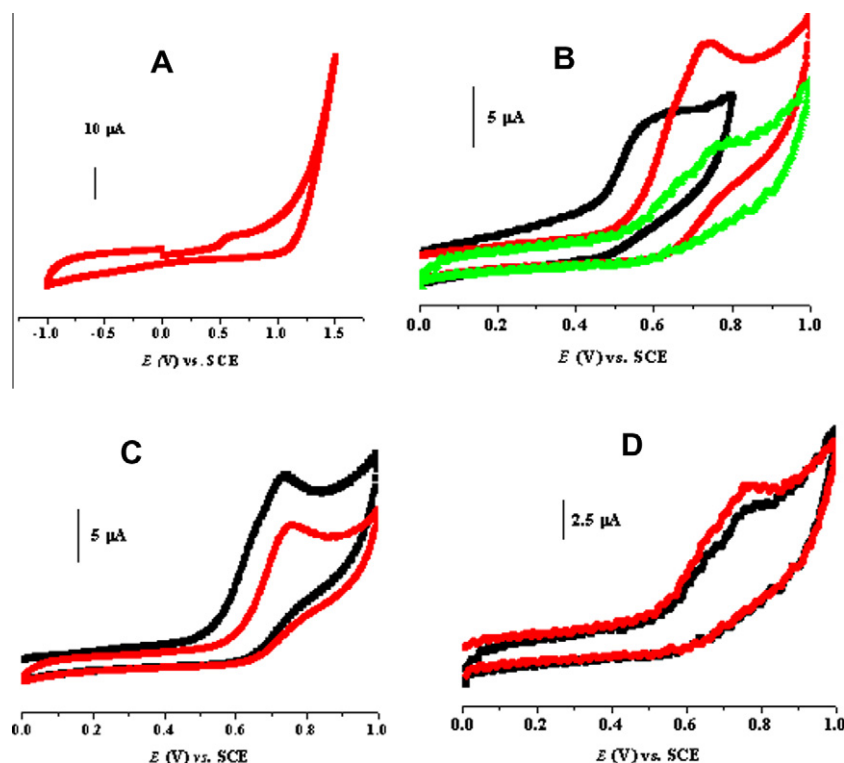

Fig. 9. (A) 1st scan CV of 0.5 mM **3** in 80% ethanol at 50 mV/s. (B) 1st scan CV's of 0.5 mM **2** (━), **2** (━) and **3** (━) in 80% ethanol at 100 mV/s. (C) 1st scan (━) and 2nd scan (━) CV's of 0.5 mM **1** 80% ethanol at 100 mV/s. (D) CVs of 0.5 mM of **3** in the absence (━) and presence (━) of 50 µM DNA at 100 mV/s.

The conductance of the ligand and its complexes was recorded in 80% ethanol at room temperature (25 °C) and fall in the range 15–19 S cm^2 mol^{-1}, suggesting their non-electrolytic nature. The results of UV–Vis spectroscopy, viscometry and cyclic voltammetry revealed an intercalative mode of interaction of these compounds with DNA as the dominant mode. The negative values of Gibb's free energy change indicate the spontaneity of these interactions. Electrochemical characterization revealed that these compounds can be irreversibly oxidized on a glassy carbon electrode, with diffusion coefficient varying in the sequence **1 > 2 > 3**.

Acknowledgments

Appendix A. Supplementary material

Crystallographic data for the structure reported in this paper has been deposited with the Cambridge Crystallographic Data Centre, CCDC 814987 for complex **3**. Copies of this information may be obtained free of charge from The Director, CCDC, 12, Union Road, Cambridge CB2 1EZ. Fax: +44 1223 336 033 or e-mail deposit@ccdc.cam.ac.uk or http://www.ccdc.cam.ac.uk.

References

[1] P. Yang, M. Guo, Metal-Based Drugs 5 (1) (1998) 41.
[2] M.H. Bhatti, S. Ali, F. Huma, S. Shahzadi, Turk. J. Chem. 29 (2005) 463.
[3] K. Shahid, S. Ali, S. Shahzadi, Z. Akhtar, Turk. J. Chem. 27 (2003) 209.
[4] E.R.T. Tiekink, App. Organomet. Chem. 5 (1991) 1.
[5] Special Issue: Recent Advances in Organotin Chemistry, Editorial, J. Organomet. Chem., 691 (2006) 1435–1436.
[6] W. Rehman, A. Badshah, S. Khan, L.T.A. Tuyet, Eur. J. Med. Chem. 44 (2009) 3981.
[7] L. Pellerito, L. Nagy, Coord. Chem. Rev. 224 (2002) 111.
[8] S. Mishra, M. Goyal, A. Singh, Main Group Met. Chem. 25 (2002) 437.
[9] A. Saxena, J.P. Tandon, A.J. Crowe, Polyhedron 4 (1985) 1085.
[10] H.L. Singh, S. Varshney, A.K. Varsheny, Appl. Organomet. Chem. 13 (1999) 637.
[11] J.S. Casas, A. Castineiras, F. Condori, M.D. Couce, U. Russo, A. Sanchez, R. Seoane, J. Sordo, J.M. Varela, Polyhedron 22 (2003) 53.
[12] R.G. Zarracino, J.R. Quinones, H. Hopfl, J. Organomet. Chem. 664 (2002) 188.
[13] B.S. Kawakami, M. Miya-Uchi, T. Tanaka, J. Inorg. Nucl. Chem. 42 (1980) 805.
[14] C. Pettiniari, F. Marchetti, R. Pettiniari, D. Martini, A. Drozdov, S. Troyanov, Inorg. Chim. Acta 325 (2001) 103.
[15] D.K. Dey, M.K. Saha, M.K. Das, N. Bhartiya, R.K. Bansal, G. Rosair, S. Mitra, Polyhedron 18 (1999) 2687.
[16] J.N.R. Ruddick, J.R. Sams, J. Organomet. Chem. 60 (1973) 233.
[17] Y. Zhou, L. Zhang, X. Zeng, J.J. Vital, X.Z. You, J. Mol. Struct. 553 (2000) 25.
[18] T.A.K. Al-Allaf, L.J. Rashan, A. Stelzner, D.R. Powell, Appl. Organomet. Chem. 17 (2003) 891.
[19] D.W. Siegmann-Louda, C.E. Carraher Jr., in: C.E. Carraher et al. (Eds.), Macromolecules Containing Metal and Metal-like Elements, Biomedical Applications, vol. 3, Wiley Interscience, New York, 2004, p. 57 (Chap. 7).
[20] Y. Ni, D. Lin, S. Kokot, Anal. Biochem. 352 (2006) 231.
[21] W.L.F. Armarego, C.L.L. Chai (Eds.), Purification of Laboratory Chemicals, 5th Edn., Butterworth-Heinemann, London, New York, 2003.
[22] Y. Zhang, X. Wang, L. Ding, Nucleosides, Nucleotides and Nucleic Acids 30 (2011) 49.
[23] C.V. Sastri, D. Eswaramoorthy, L. Giribabu, B.G. Maiya, J. Inorg. Biochem. 94 (2003) 138.
[24] J. Ahlers, Biochem. J. 149 (1975) 535.
[25] K. Jiao, W. Sun, H.Y. Wang, Chinese Chem. Lett. 13 (1) (2002) 69.
[26] K. Walter, C. Schütt, in: H.U. Bergmeyer (Ed.), Methods of Enzymatic Analysis, vol. 2, Academic Press Inc., New York, 1974, p. 860.
[27] A. Rehman, M.I. Choudhary, W.J. Thomsen, Bioassay Techniques for Drug Development, Harwood Academic Publishers, Amsterdam, The Netherlands, 2001. p. 9.
[28] B.N. Mayer, N.R. Ferrigni, J.E. Putnam, L.B. Jacobson, D.E. Nichols, J.L. Mclaughlin, Planta Med. 45 (1982) 31.
[29] T. Sedaghat, F. Jalilian, J. Iran. Chem. Soc. 6 (2) (2009) 271.
[30] T. Sedaghat, S. Menati, Inorg. Chem. Commun. 7 (2004) 760.
[31] S.B. Kumar, S. Bhttacharyya, S.K. Dutta, E.R.T. Tiekink, M. Chaudhury, J. Chem. Soc., Dalton Trans. (1995) 2619.
[32] A. Graisa, Y. Farina, E. Yousif, E.E. Saad, Int. J. Chem. 1 (2) (2009) 34.
[33] E. Saad, Y. Farina, I. Baba, H. Othman, Sains Malaysiana 32 (2003) 79.
[34] B. Yearwood, S. Parkin, D.A. Atwood, Inorg. Chim. Acta 333 (2002) 124.
[35] Z. Popovic, V. Roje, G. Pavlovic, D. Matkovic-Calogovic, G. Giester, J. Mol. Struct. 597 (2001) 39.
[36] S.G. Teoh, S.B. Teo, G.Y. Yeap, J.P. Declercq, Polyhedron 10 (1991) 2683.
[37] T.P. Lockhart, W.F. Manders, Inorg. Chem. 25 (1986) 892.
[38] T.P. Lockhart, W.F. Manders, J.J. Zuckerman, J. Am. Chem. Soc. 107 (1985) 4546.
[39] A. Lycka, M. Nadvornik, K. Handlir, J. Holecek, Collect. Czech. Chem. Commun. 49 (1984) 2903.
[40] J. Holecek, M. Nadvornik, K. Handlir, A. Lycka, J. Organomet. Chem. 315 (1986) 299.
[41] V. Pejchal, J. Holecek, M. Nadvornik, A. Lycka, Collect. Czech. Chem. Commum. 60 (1995) 1492.
[42] J. Holecek, A. Lycka, K. Handlir, M. Nadvornik, Collect. Czech. Chem. Commun. 55 (1990) 1193.
[43] F. Kayser, M. Biesemans, A. Boualam, E.R.T. Tiekink, A. ElKhloufi, J. Meunier-Piret, A. Bouhdid, K. Jurkschat, M. Gielen, R. Willem, Organometallics 13 (1994) 1098.
[44] D. Dakternieks, A. Duthie, D.R. Smyth, C.P.D. Stapleton, E.R.T. Tiekink, Organometallics 22 (2003) 4599.
[45] F.P. Pruchnik, M. Banbula, Z. Ciunik, M. Latocha, B. Skop, T. Wilczok, Inorg. Chim. Acta 356 (2003) 62.
[46] A.W. Addison, T.N. Rao, J. Reedijk, J. van Rijn, G.C. Verschoor, J. Chem. Soc., Dalton Trans. 7 (1984) 1349.
[47] F. Ahmad, S. Ali, M. Parvez, A. Munir, M. Mazhar, K.M. Khan, T.A. Shah, Heteroatom Chem. 13 (2002) 638.
[48] T.S.B. Baul, S. Dutta, E. Rivarola, R. Butcher, F.E. Smith, J. Organomet. Chem. 654 (2002) 100.
[49] S. Shujha, A. Shah, Z. Rehman, N. Muhammad, S. Ali, R. Qureshi, N. Khalid, A. Meetsma, Eur. J. Med. Chem. 45 (2010) 2902.
[50] C.Y. Zhou, J. Zhao, Y.B. Wu, C.X. Yin, P. Yang, J. Inorg. Biochem. 101 (2007) 10.
[51] N. Li, Y. Ma, C. Yang, L. Guo, X. Yang, Biophys. Chem. 116 (2005) 199.
[52] C.C. Ju, A.G. Zhang, C.L. Yuan, X.L. Zhao, K.Z. Wang, J. Inorg. Biochem. 105 (435) (2011) 443.
[53] V. Gonzalez-Ruiz, A.I. Olives, M.A. Martin, P. Ribelles, M.T. Ramos, J.C. Menendez, Biomedical Engineering, Trends, Research and Technologies, InTech, India, 2011. p. 65 (ISBN 978-953-307-514-3).
[54] J.L. Garcia-Gimenez, M. Gonzalez-Alvarez, M. Liu-Gonzalez, B. Macias, J. Borras, G. Alzuet, J. Inorg. Biochem. 103 (2009) 923.
[55] D. Li, J. Tian, W. Gu, X. Liu, S. Yan, J. Inorg. Biochem. 104 (2010) 171.
[56] J.L. Garcia-Gimenez, G. Alzuet, M. Gonzalez-alvarez, M. Liu-Gonzalez, A. Castineiras, J. Borras, J. Inorg. Biochem. 103 (2009) 243.
[57] M. Jiang, Y. Li, Z. Wu, Z. Liu, C. Yan, J. Inorg. Biochem. 103 (2009) 833.
[58] M.R. Malik, V. Vasylyeva, K. Merz, N. Metzler-Nolte, M. Saleem, S. Ali, A.A. Isab, K.S. Munawar, S. Ahmad, Inorg. Chim. Acta 376 (2011) 207.
[59] F.J. Huoa, C.X. Yin, Y.B. Wu, P. Yang, Russ. J. Inorg. Chem. 55 (7) (2010) 1087.
[60] A. Chaudhary, R.V. Singh, Relat. Elem. 178 (2003) 603.
[61] K.S. Prasad, L.S. Kumar, S.C. Shekar, M. Prasad, H.D. Revanasiddappa, Chem. Sci. J. 12 (2011) 1.
[62] T.D. Thangadurai, K. Natarajan, Trans. Met. Chem. 26 (4–5) (2001) 500.
[63] N. Dharmaraj, P. Viswanathamurthi, K. Natarajan, Trans. Met. Chem. 26 (1–2) (2001) 105.
[64] R.P. John, A. Sreekanth, V. Rajakannan, T.A. Ajith, M.R.P. Kurup, Polyhedron 23 (2004) 2549.
[65] W. Rehman, M.K. Baloch, A. Badshah, Eur. J. Med. Chem. 43 (2008) 2380.
[66] A. Silvestri, G. Ruisi, R. Barbieri, Hyperfine Interac 126 (2000) 43.
[67] A.J. Bard, L.R. Faulkner, Electrochemical Methods Fundamentals and Applications, 2nd ed., Wiley, New York, 2001. p. 494.
[68] C.M.A. Brett, A.M.O. Brett, Electrochemistry principles, methods and applications, Oxford University Press, UK, 1993.